Journal of Science and Technology in Civil Engineering, HUCE (NUCE), 2022, 16 (4): 73–86

BLAST TESTING OF ULTRA-HIGH PERFORMANCE CONCRETE FORTIFICATIONS USING LOCAL MATERIALS

Pham Manh Hao[a], Nguyen Cong Thang[b,*], Nguyen Van Thao[a], Nguyen Van Tuan[b],

Luong Nhu Hai[a], Ngo Ngoc Thuy[c], Nguyen Xuan Man[d]

[a] *Center for High Technology Development, Vietnam Academy of Science and Technology,*
18 Hoang Quoc Viet road, Cau Giay district, Hanoi, Vietnam
[b] *Faculty of Building Materials, Hanoi University of Civil Engineering,*
55 Giai Phong road, Hai Ba Trung district, Hanoi, Vietnam
[c] *Institute of Techniques for Special Engineering, Le Quy Don Technical University,*
236 Hoang Quoc Viet road, Cau Giay district, Hanoi, Vietnam
[d] *Faculty of Civil Engineering, Hanoi University of Mining and Geology,*
18 Vien street, Bac Tu Liem district, Hanoi, Vietnam

Article history:
Received 15/9/2022, Revised 28/9/2022, Accepted 29/9/2022

Abstract

This paper presents experimental results on blast testing of fortifications made from ultra-high performance concrete (UHPC) and ordinary concrete (NC) by a non-contact explosion test with the TNT explosive. UHPC and NC samples used in the test were of the type of precast fortification of the real-scale and structure. TNT explosive was used in the test with a mass of 600 g per detonation. The explosive charge was centered on the top of fortifications, with the distance from the center of the explosion to the top of the fortification roof being 600 mm, 450 mm, and 300 mm, respectively. The test results, i.e., the strain of fortification roof elements, the explosive load resistance, and the destruction level, were evaluated by comparing the UHPC and NC fortifications.

Keywords: fortifications; ultra-high performance concrete; explosive load; damage area; strain.

https://doi.org/10.31814/stce.nuce2022-16(4)-06

---

1. Introduction

Reinforced concrete (RC) is one of the world's most widely used building materials for primary load-bearing construction structures. With the development of science and technology, RC has gradually been applied in defense and security works, especially fortifications. In addition, the possibility of absorbing and suppressing energy caused by explosive pressure by high-strength concrete is also of great interest for the design and building of defense works [1]. An explosion, whether accidentally or intentionally near the works, will have significant consequences, although low probability. Explosive loads occurring with high intensity and short duration will release a large energy source in the form of explosive waves. The pressure of these explosive waves will act directly on the structure, causing

*Corresponding author. *E-mail address:* thangnc@huce.edu.vn (Thang, N. C.)

the destruction of materials and structures, which can lead to the complete collapse of the structure [2–4]. Concrete debris generated after an explosion will have a high speed that can cause casualties and damage to people and property. In order to minimize the damage of explosive loads, it is essential to study the mechanical behavior of concrete under the impact of explosive loads, especially with structures made from ultra-high performance concrete.

Ultra-high performance concrete referred to as UHPC is a new material researched and developed in the world since the 1990s [5, 6] with outstanding characteristics such as very high compressive strength (from 120 to over 200 MPa) [2, 7], high bending and shear resistance, impact resistance, very high fatigue load and especially long-term durability and stability. UHPC is a high-tech material with new technological characteristics related to its composition. Mechanical behaviors, calculation formulas, and engineering and design guidelines have been published in France, USA, and Germany [2, 6, 8]. Several early applications in Canada, Europe, Asia, and the US demonstrated the benefits of this new material in terms of cost, sustainability, and many other outstanding features. However, the current research works on applying UHPC in the world have only focused on civil works such as bridges, roads, high-rise buildings, traffic tunnels, hydroelectricity, etc., however not much research has been focused on the application of UHPC for military and defense projects. In Vietnam, UHPC has been studied for the past 20 years [9–13], and initially, there have been studies with thin formwork structures, explosive load-bearing structures with emulsion explosives, and contact explosives in the direction of application in defense projects [14–16].

In addition to the requirements of explosive and piercing resistance, the fortifications must also ensure high moisture resistance, corrosion resistance, and heat resistance. These parameters of UHPC are entirely superior to that of conventional concrete. In addition, the world's research on UHPC for military applications is still in the experimental stage, with guidelines, recommendations for each region, available material conditions, and specific materials and test methods. Many significant issues that need to be studied in depth, such as the effects of shrinkage, creep, and advanced countries in the world are still studying explosion capacity, etc. Thus, it can be seen that the research on the features and application scope of UHPC still needs to be implemented more deeply, and the scope of application also needs to be expanded, especially the application in Security-Defense.

This paper presents the experimental results on the possibility of explosive load resistance of fortification samples made of UHPC compared with the samples made of conventional concrete with compressive strength of 30 MPa. Based on these experimental results, some very important parameters were determined, such as deformation characteristics and load-bearing ability of fortifications under the impact of explosive loads at different distances.

2. Materials and methods

2.1. Materials

Materials used to produce UHPC include quartz sand (S) with particle size from 100 - 300 μm, bulk density of 1460 kg/m^3, dry surface saturation moisture of 1.1%; the cement (C) used in the study is Portland cement PC40; undensified silica fume (SF) from Elkem company with SiO_2 content reaching over 92%, mean particle size is 0.15 μm; Fly ash (FA) used is from Pha Lai thermal power plant with a strength reactivity index of 93.4%; the superplasticizer (SP) used in the study has a polycarboxylate based with a dry solid content of 30%; dispersed steel fiber (F) with Dramix type, having the diameter d = 0.2 mm, the length l = 13 mm (the l/d ratio of 65), the tensile strength is 2750 MPa. Besides, fine aggregate (S) and coarse aggregate (CA) have technical properties that are in accordance with TCVN 7570:2006 [17].

Table 1. Some properties of Portland cement PC40

Properties	Unit	Value	Specification
Retained on 0.09 mm sieve	%	0.6	≤ 1.0
Fineness (Blaine)	cm^2/g	3870	≥ 2800
Standard consistency	%	29.5	-
Compressive strength	MPa		
- 3 days		29.8	≥ 21.0
- 28 days		52.2	≥ 40.0

2.2. *Mix proportions and properties of concrete*

In the study, two types of concrete were used, i.e., conventional concrete of grade M30 (B22.5) and UHPC with compressive strength above 140 MPa. With UHPC, steel fiber was used with a content of 2% by volume of the concrete mix. The composition of the concrete used is given in Table 2.

Table 2. Mix proportion of concrete mixtures

Sign	Ingredients of the concrete mixture (kg/m^3)							Fiber, % by vol.
	Sand	Coarse aggregate	C	FA	SF	SP	W	
B22.5	780	1060	360				175	
UHPC	1100		770	220	110	11	189	2

The mechanical properties of B22.5 concrete and UHPC are given in Table 3. It is noted that tensile strength in bending of concrete (flexural strength) was measured with a simple beam with third-point loading according to ASTM C1609 standard.

Table 3. Mechanical properties of concrete

Sample	Compressive strength (MPa)	Flexural strength (MPa)	Elastic modulus (GPa)
B22.5	30	3	30
UHPC	140	15	50

2.3. *The fortification model used for blast testing*

The selected fortification model is the fortification type assembled from CB-23 members (beams) and CB-24 members (pillars). Details of the CB-23 member and CB-24 member design are shown in Fig. 1. These elements were assembled and linked together by bolted connection details to ensure the stability of the fortifications during work. The test fortification model was assembled from five CB-23 and ten CB-24 elements. Detailed cross sections of fortifications assembled by concrete elements are shown in Fig. 3.

The detailed reinforcement layout of the horizontal element CB-23 is provided in Fig 2.

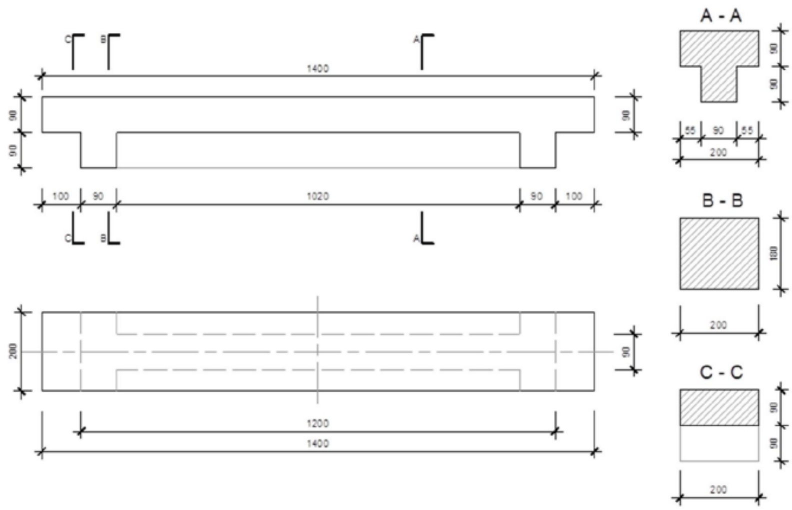

(a) The details of CB-23

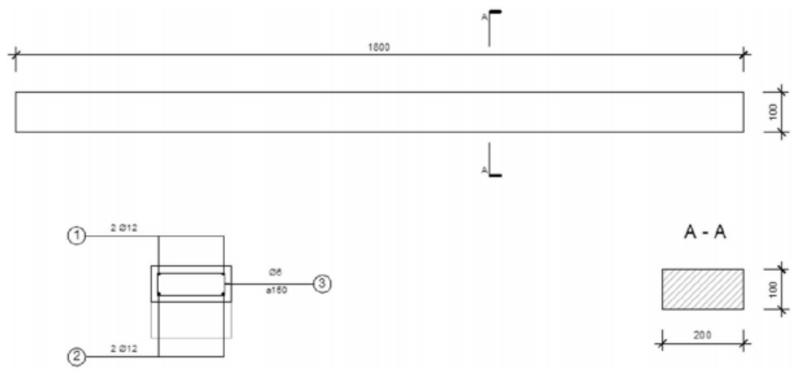

(b) The details of CB-24

Figure 1. Details of the designed element of fortification

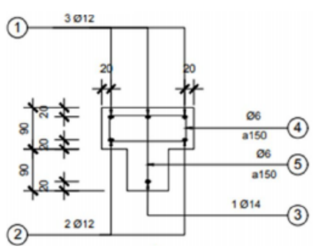

(a)

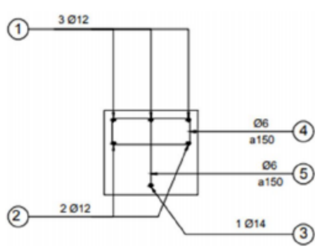

(b)

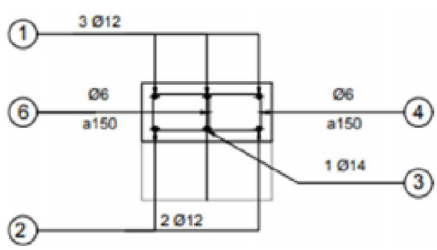

(c)

Figure 2. Detailed reinforcement layout of the horizontal element CB-23

The testing process was conducted on the fortification models with the same structure and size, including one UHPC model and the B22.5 concrete model for control (Fig. 3). The details of connections between the vertical and horizontal elements (CB-23 and CB-24) is provided in Fig. 4.

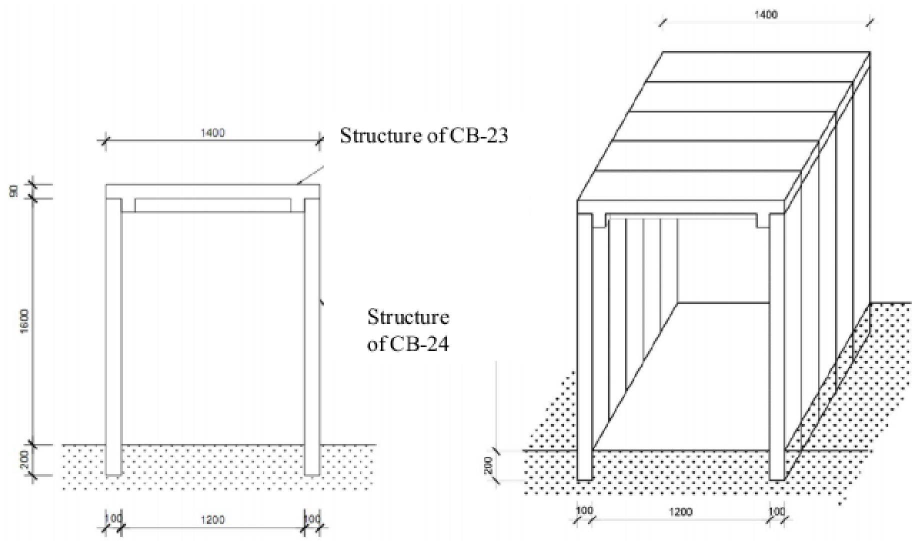

Figure 3. Cross section of fortifications assembled by concrete elements and fortification model being assembled from thereof

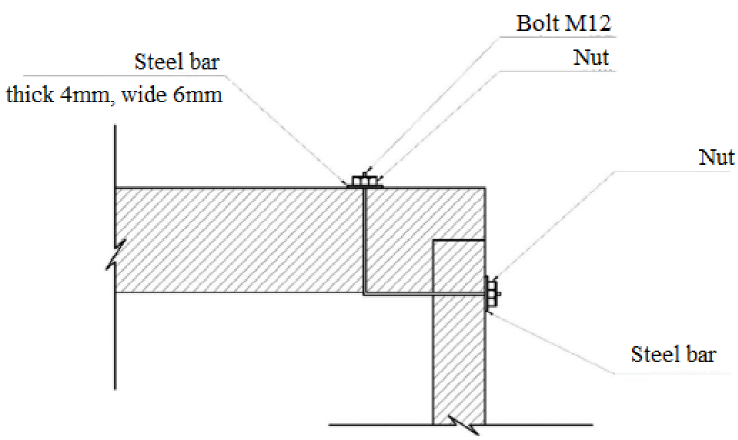

Figure 4. The details of connections between the vertical and horizontal elements (CB-23 and CB-24)

2.4. Design the blast testing plan

The explosive charge of each explosion was 600g of TNT, equivalent to an 82 mortar shell, was prepared for the blast testing plan for fortifications made of UHPC and the B22.5 concrete. The location to place the explosive is in the middle above the roof of the fortification. The explosion distance was designed with 600 mm, 450 mm, and 300 mm to investigate the explosive load resistance of the fortifications. The layout design model of the explosive charge is shown in Fig. 5. The inside surface of the roof elements opposite the location of the explosive charge was attached with a sensor (strain gauge) to measure the strain of the structure when subjected to explosive loads. The strain gauge of the fortification is shown in Fig. 6.

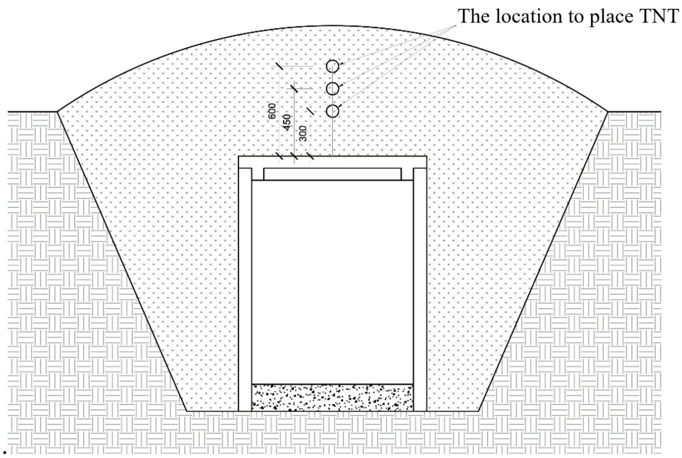

Figure 5. The layout of placing TNT explosives for field testing

Figure 6. Arrangement of strain gauges on fortification roof elements

The models of UHPC (a) and B22.5 (b) fortifications installed for the blast testing at the site are shown in Fig. 7.

(a) UHPC

(b) B22.5

Figure 7. Models of fortifications installed in the blast test site

2.5. Recording the strain

The instrument (datalogger) was used to record strain with very short time intervals in this study including multi channel dynamic meter NI cRIO-9137 (Fig. 8) and strain gauge PL-60 (Fig. 9).

Figure 8. Multichannel dynamic meter NI cRIO-9137

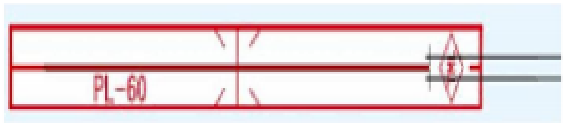

Figure 9. Strain gauge PL-60

3. Research results and discussion

3.1. Explosive load resistance of the B22.5 concrete fortifications

a. TNT explosive charge placed above the roof of fortifications at a distance of 600 mm

The test was carried out with an explosive charge of 600 g of TNT placed at a distance of 600 mm from the center of the explosion to the roof of the fortifications. The strain value of the fortification roof elements of normal concrete B22.5 corresponding to the distance, i.e., 600 mm, 632 mm, and 721 mm were measured corresponding to the distance from the explosion center to the roof elements, i.e., the distance to the element 1 is 600 mm, to the element 2 is 632 mm, and to the element 3 is 721 mm respectively. Roof elements for fortifications with numbers 1, 2, and 3 are arranged as shown on the left Fig. 6 and are fitted with a strain gauge (deformation sensor) to measure strain, as shown on the right Fig. 6. As a result, after detonating an explosive charge of 600 g from the above distance, the roof elements of the fortifications, particularly the entire fortification structure, ensure stability. The chart shows that, at the time of detonation, which is recorded at position 1s on the time axis, the roof elements of the fortifications are subject to a rather large instantaneous deformation, with a strong amplitude of vibration along both positive and negative directions. The maximum strain value is +0.00167 (Fig. 10), +0.00123 (Fig. 11), and +0.00100 (Fig. 12) for roof elements 1, 2, and 3, respectively. After the moment of instantaneous deformation mentioned above, the roof elements quickly returned to a stable equilibrium with a horizontal graph parallel to the time axis. However, these graphs do not return to the original position as before detonation (with zero strain), but all have

Table 4. The largest strain value of the roof elements with TNT explosive charge of 600g placed at 0.600 m from the roof of the fortifications of the B22.5 concrete

No	Element	Distance from measuring point to explosion center (m)	Maximum strain value (mm/mm)	Deviation
1	Roof element 1	0.600	0.0016671	0.00167
2	Roof element 2	0.632	0.0012257	0.00123
3	Roof element 3	0.721	0.0010247	0.00100

a residual strain with a value greater than 0. This value is about 0.0004, 0.00025, and 0.0002 for the roof elements 1, 2, and 3, respectively. Visually, it can be seen that the roof elements and the entire fortification structure generally were still in a normal state, and no cracks were observed.

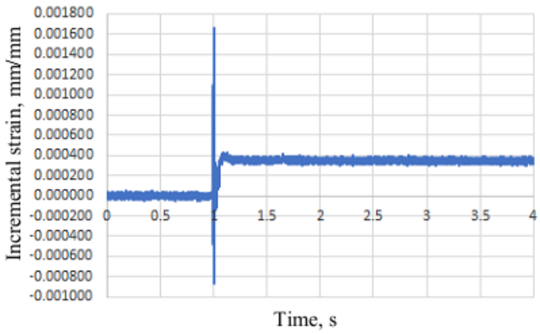

Figure 10. Incremental strain of roof element 1 of B22.5 concrete fortifications

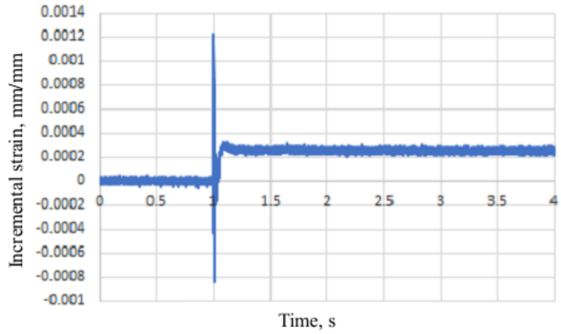

Figure 11. Incremental strain of roof element 2 of B22.5 concrete fortifications

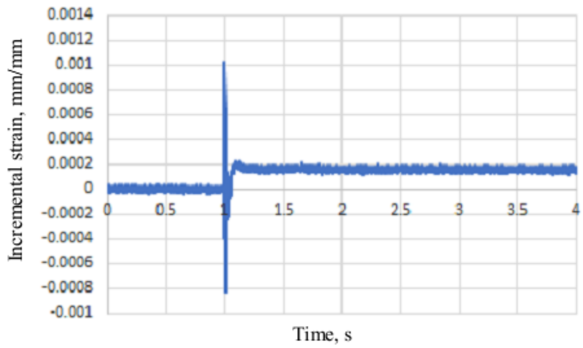

Figure 12. Incremental strain of roof element 3 of B22.5 concrete fortifications

b. TNT explosive charge placed above the roof of fortifications at a distance of 450 mm

The explosive charge of 600 g of TNT is placed at a distance of 450 mm from the center of the explosion to the top of the fortifications. At that time, the distances from the explosion center to the roof elements with a strain gauge attached to roof elements 1, 2, and 3 were 450 mm, 490 mm, and 600 mm, respectively. As a result, the roof element 1 of the fortifications was deformed, cracked, and destroyed (Fig. 13). Roof elements 2 and 3 were stable, with a few small cracks, but normal strain was still measured (Fig. 14 and Fig. 15). However, the fortification roof's general structure was considered unstable and could no longer bear the load due to one member being destroyed.

The results of the strain measurement of roof elements of the B22.5 concrete fortifications subjected to the explosive load of 600 g TNT explosives placed at 450 mm from the top of the fortification roof are shown in Table 5.

From the results obtained above, it can be concluded that, with the explosive charge of 600 g of TNT placed at the distance of 600 mm from the explosion center to the roof of the fortifications made of ordinary concrete B22.5, the fortification structure is stable, with no signs of destruction.

Figure 13. The image of the roof elements of the B22.5 fortifications being destroyed

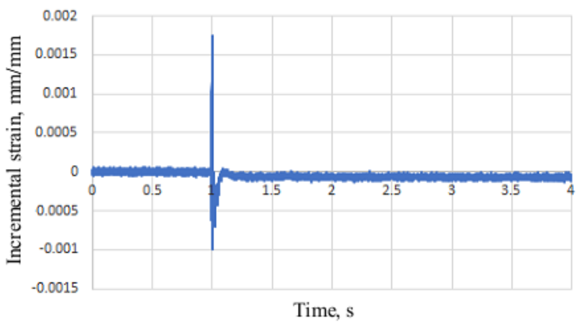

Figure 14. Incremental strain of roof element 2 of B22.5 concrete fortifications

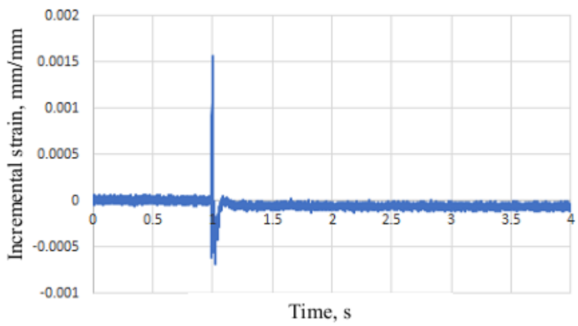

Figure 15. Incremental strain of the roof element 3 of B22.5 concrete fortifications

Table 5. The maximum strain value of the roof elements with an explosive charge of 600 g placed 0.45 m from the roof of ordinary concrete fortifications

No	Element	Distance from measuring point to explosion center (mm)	Maximum strain value (mm/mm)	Deviation
1	Roof element 1	0.450	Impossible to measure	-
2	Roof element 2	0.492	0.0017514	0.00175
3	Roof element 3	0.602	0.0015614	0.00156

The relative deformation of the roof elements has been measured, with the maximum strain value of the roof elements (member CB-23) being from 0.00100 to 0.00167. Meanwhile, with 600 g of TNT explosive charge placed at 450 mm from the center of the explosion to the roof of the B22.5 concrete fortifications, the fortification structure was unstable, and a roof element was destroyed. Other elements also cracked with horizontal fractures in the middle. As a result, the fortifications lost their load-carrying capacity, and no deformation could be measured.

3.2. The explosive load resistance of the UHPC fortifications

a. TNT explosive charge placed on the fortification roof at a distance of 600 mm

When detonated with 600 g of TNT, the distance from the center of the explosion to the top surface of the fortifications is 600 mm. The distance from the center of the explosion to the measuring point to roof elements 1, 2, and 3 is 600 mm, 632 mm, and 721 mm, respectively. The strain curve of UHPC fortification roof elements when subjected to explosive loads is shown in Fig. 16 to Fig. 18.

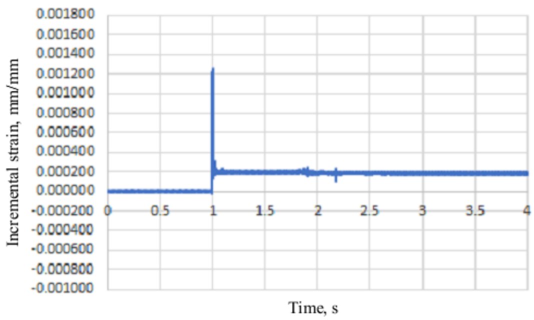

Figure 16. Incremental strain of the roof element 1 of UHPC fortifications at a distance of 600 mm to the explosion center

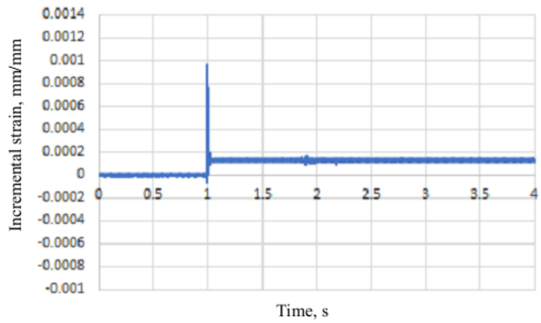

Figure 17. Incremental strain of roof element 2 of UHPC fortifications at a distance of 632 mm to explosion center

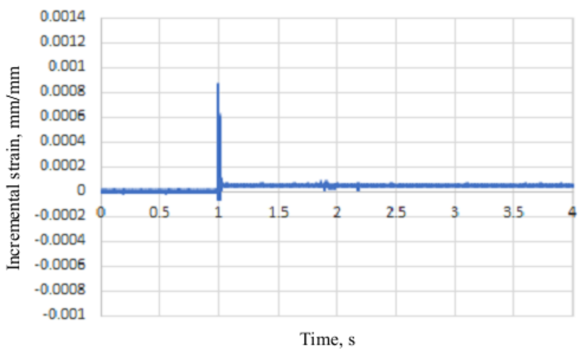

Figure 18. Incremental strain of roof element 3 of UHPC fortifications at a distance of 721 mm to explosion center

The maximum strain value of fortification roof elements (CB-23) recorded in this test is shown in Table 6.

Table 6. The maximum strain value of the UHPC fortification roof elements with an explosive charge of 600 g placed at 600 mm from the fortification roof

No	Element	Distance from measuring point to explosion center (mm)	Maximum strain value (mm/mm)	Deviation
1	Roof element 1	600	0.0012667	0.00127
2	Roof element 2	632	0.0009738	0.00097
3	Roof element 3	721	0.0008668	0.00087

The results of measuring the strain of the roof elements made of ultra-high performance concrete (UHPC) when subjected to the load of 600 g TNT explosive charge placed at the center, at 600 mm from the top of the fortification roof showed that, at the time of detonation, the roof elements have instantaneous deformation with the largest relative strain value varying from 0.00087 to 0.00127. Immediately after that, the roof elements returned to equilibrium with the strain graph parallel to the time axis with a very small residual strain value, less than 0.0002. This shows that the roof structures of the fortifications are almost kept to their original steady state, with no signs of destruction due to explosive load.

b. TNT explosive charge placed on the fortification roof with a distance of 450 mm

The results after the explosion show that the UHPC fortification structure still ensures bearing safety. The strain gauges have measured and recorded the strain value of the roof elements of the fortifications. The strain curves of the roof elements 1, 2, and 3 are shown in Fig. 19, Fig. 20, and Fig. 21, respectively. The maximum strain value recorded for the roof elements in this test is shown in Table 7.

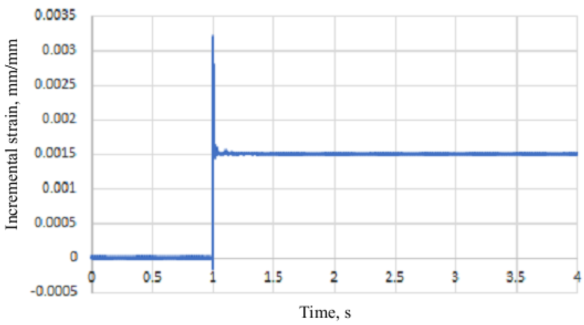

Figure 19. Incremental strain of roof element 1 at a distance of 450 mm to explosion center

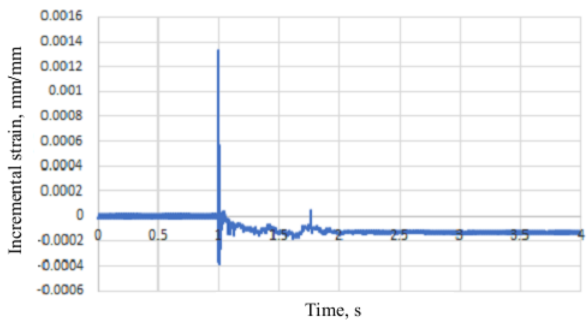

Figure 20. Incremental strain of roof element 2 at a distance of 492 mm to explosion center

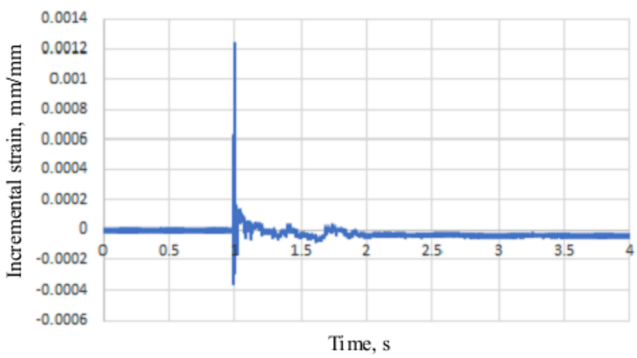

Figure 21. Incremental strain of roof element 3 at a distance of 602 mm to explosion center

Table 7. Maximum strain value of UHPC fortification roof elements with 600 g explosive load placed 450 mm from the fortification roof

No	Element	Distance from measuring point to explosion center (mm)	Maximum strain value (mm/mm)	Deviation
1	Roof element 1	450	0.0032134	0.00321
2	Roof element 2	492	0.0013307	0.00133
3	Roof element 3	602	0.0012328	0.00123

c. TNT explosive charge placed on the fortification roof at a distance of 300 mm

When detonating 600 g of TNT at a distance of 300 mm from the center of the explosion to the roof of the fortifications, the structure of the roof of UHPC fortifications was deformed, and some cracks appeared in the middle of the roof elements. The strain gauges are detached, and strain can not be measured (Fig. 22). However, the fortifications still retain stability and are still capable of carrying loads.

Figure 22. Image of UHPC fortification roof elements after exploding at a distance of 300 mm

4. Conclusions

Based on the experimental results, some conclusions can be drawn as follows:

The possibility of the fortifications to withstand explosive loads varies markedly. At the same test distance, the UHPC fortification has a very small residual strain, and the NC fortification is very large.

In case of an explosive charge of 600 g of TNT placed at a distance of 600 mm from the center of the explosion to the nearest point in the center of the roof-top of the fortifications, the fortification models are both stable and capable of withstanding explosive loads. The most significant relative strain value of the UHPC fortification roof element nearest to the center of explosion measured at the time of detonation is 18.23% less than that of the corresponding element made of B22.5 concrete, and for the roof elements farthest to the center of the explosion, that difference is 31.61%. In addition, the closer the measured strain to the explosion center, the more significant the difference between the two types of materials. The residual strain value also shows a clear difference in strain versus time.

In case of an explosive charge of 600 g of TNT placed at a distance of 450 mm from the center of the explosion to the nearest point in the center of the top of the fortifications, the UHPC fortifications are stable, with no signs of destruction (no cracks, strain value is measured and recorded). In contrast, in the B22.5 concrete fortification model, the roof elements were cracked and destroyed, had one destroyed roof element, and no deformation was measured. Other elements were cracked in the middle, and fortification structure, in general, loses its load-bearing capacity and is unable to serve for the next blast test.

In case of an explosive charge of 600 g TNT placed at a distance of 300 mm from the center of the explosion to the nearest point in the center of the roof of the UHPC fortifications, the fortification roof structure was deformed, forming horizontal cracks in the middle of the elements, the strain gauge was detached, and the strain value could not be measured. However, the fortification structure, in general, still retains its stability and load-bearing capacity.

Acknowledgment

The authors would like to thank the Ministry of Science and Technology for funding the national science and technology task under code number ĐTĐLCN.37/18; The Center for High Technology Development - HTD (in charge of performing the task), Hanoi University of Civil Engineering, and the Military Technical Academy, which have created favorable conditions for the authors to complete this research.

References

[1] Ta, N. T., Loi, V. D., Dich, D. V. (1995). *Textbook of fortifications*, volume 1. Military Technical Institute. (in Vietnamese).

[2] ACI 239R-18 (2018). *Ultra-high-performance concrete: An emerging technology report, in emerging technology series*. American concrete Institute: ISBN: 978-1-64195-034-3, p. 25.

[3] Cheyrezy, M., Maret, V., Frouin, L. (1995). Microstructural analysis of RPC (Reactive Powder Concrete). *Cement and Concrete Research*, 25(7):1491–1500.

[4] Nguyen, C. T., Pham, H. H., Nguyen, V. T., Pham, S. D., Cu, V. H. (2020). Evaluating the effect of steel fibers on some mechanical properties of ultra-high performance concrete. In *Lecture Notes in Civil Engineering*, Springer Singapore, 493–501.

[5] Richard, P., Cheyrezy, M. (1995). Composition of reactive powder concretes. *Cement and Concrete Research*, 25(7):1501–1511.

[6] AFGC-SETRA (2002). *Ultra high performance fibre-reinforced concretes (UHPFRC)-state of the art*. AFGC Publication, Paris, France.

[7] ASTM C1856-2017 (2017). *Standard practice for fabricating and testing specimens of ultra-high performance concrete*. ASTM International, West Conshohocken, Pennsylvania, USA.

[8] Schmidt, M., Fehling, E. (2005). Ultra-high-performance concrete: research, development and application in Europe. *ACI Special Publication*, 228(1):51–78.

[9] Thang, N. C., Hanh, P. H., Tuan, N. V. (2013). Ultra High Performance Concrete using the combination of silica fume and fly ash available in Vietnam. *Journal of Science and Technology in Civil Engineering (STCE) - HUCE*, 15:83–92. (in Vietnamese).

[10] Thang, N. C., Tuan, N. V., Yang, K.-H., Phung, Q. T. (2020). Effect of zeolite on shrinkage and crack resistance of high-performance cement-based concrete. *Materials*, 13(17):3773.

[11] Tuan, N. V., Thang, N. C., Hanh, P. H. (2015). Sustainable development of Ultra-High Strength Concrete using mineral admixtures to partly replace cement in Vietnam. *Journal of Science and Technology in Civil Engineering (STCE) - HUCE*, 24:11–18. (in Vietnamese).

[12] Dong, P. S., Tuan, N. V., Thanh, L. T., Thang, N. C., Cu, V. H., Mun, J.-H. (2020). Compressive strength development of high-volume fly ash ultra-high-performance concrete under heat curing condition with time. *Applied Sciences*, 10(20):7107.

[13] Tuan, N. V., Phung, Q. T., Seetharam, S., Thang, N. C. (2022). Synergistic effects of ground granulated blast furnace slag and silica fume on the hydration and compressive strength of extremely low w/b ratio cement pastes. *Materials Today Communications*, 33:104531.

[14] Danh, L. B., Hoa, P. D., Thang, N. C., Linh, N. D., Dung, B. T. T., Loc, B. T., Dat, D. V. (2019). Experimental study of Ultra-high Performance Concrete (UHPC) Slabs under contact explosions. *Journal of Science and Technology in Civil Engineering (STCE) - HUCE*, 13(3V):12–21. (in Vietnamese).

[15] Hao, P. M., Tuan, N. V., Thang, N. C., Thao, N. V., Hai, L. N., Dong, P. S., Man, N. X., Thuy, N. N. (2020). Effect of carbon nanotubes on the chloride penetration in ultra-high-performance concrete. In *Lecture Notes in Civil Engineering*, Springer International Publishing, 69–80.

[16] Nghia, H. T., Thang, N. C., Tuan, N. V., Hung, C. V., Yang, K. H., Dong, P. S. (2021). Experimental study to produce manhole cover using ultra-high performance concrete. Geotechnique, construction materials and environment. *International Journal of GEOMATE*, 21(85).

[17] TCVN 7570:2006. *Aggregates for concrete and mortar- Specifications*. Ministry of Science and Technology. (in Vietnamese).